Hinode-3: The 3rd Hinode Science Meeting
ASP Conference Series, Vol. 454
T. Sekii, T. Watanabe, and T. Sakurai eds.

Structure of Small Magnetic Elements in the Solar Atmosphere

Vicente Domingo,[1] Judith Palacios,[1] Laura A. Balmaceda,[2]
Santiago Vargas Domínguez,[3] and Iballa Cabello[1]

[1]*Image Processing Laboratory, Universidad de Valencia, P.O. Box 22085, E-46071, Valencia, Spain*

[2]*Inst. de Ciencias Astronómicas, de la Tierra y del Espacio - ICATE, CONICET, Av. España 1512 Sur, 5400 San Juan, Argentina*

[3] *Mullard Space Science Laboratory, University College London, Holmbury St Mary, Dorking, Surrey, RH5 6NT, UK*

Abstract. High resolution images at different wavelengths, spectrograms and magnetograms, representing different levels of the solar atmosphere obtained with Hinode have been combined to study the 3-dimensional structure of the small magnetic elements in relation to their radiance. A small magnetic element is described as example of the study.

1. Introduction

The small magnetic elements have been studied profusely, see for instance the review paper by de Wijn et al. (2009). However, many essential characteristics remain contradictory regarding different studies. At the beginning of the 70s, several studies started to indicate that most of the magnetic flux outside active regions was contained in subresolution kilogauss elements. This conclusion derived in the thin tube flux model (Spruit 1976; Parker 1976) making these unresolved structures the building block or element in the photosphere. However, these features can appear in the shape of thin sheet (Berger et al. 2004) may be composed of smaller tubes, or tubes that can be structured as a bunch of slender tubes (Sánchez Almeida 1997); they appear in every environment in the solar photosphere. These structures appear as facular brightening, G-band bright points, filigree. In this work we focus on G-band bright points analysis. G-band bright points, GBP, are bright in G-band because inside the small magnetic tube, lateral heating provokes differential CH dissociation, that makes the opacity lower and the tube brighter (Kiselman et al. 2001). These bright points were also observed in CN band, their contrast calculated and compared with G-band in filter bandwidth dependence and MHD modeling by Uitenbroek & Tristchler (2006). In the case of the GBPs, the detection, size and coverage are usually calculated by the use of segmentation algorithms, which detect high contrast above a threshold, separate from the structure where they are embedded (an inter-granular lane or close to a granule) and merge the structure. A related study, in a joint campaign with the SST of La Palma, uses Hinode CN filter-grams and Mg I magnetograms, close to the disk center, on September, 29 2007, and SST G-band data. MLT4 segmentation code of Bovelet and Wiehr (2007)

was applied to CN images, and the segmentation code used in Sánchez Almeida et al. (2004) was used for G-band SST images, finding that the area coverage is 0.22 for G-band, 0.26 for CN (Balmaceda et. al. 2009).

2. Observations

We use two Hinode data sets in three different wavelengths plus the SOT-SP (Spectro-polarimeter) data. One data set, obtained in 2008, Aug 6, from 08:02:56 to 09:17:05 UT, consists on CN (λ=388.3nm), Ca II(λ=396.8nm), G-band(λ= 430.56 nm) images, SP scans, centered in μ=0.85 (491",-14"). The second data set, from 2008, Aug 7, from 08:01:24 to 09:06:59 UT, is similar, but also with one Na I magnetogram in the blue wing of the Na I line (λ= 589.6 nm) and centered in μ=0.86, at coordinates (-8",485"). The Broadband Filter (BFI) has a FOV of 55"75 $\times$ 55"75, the SP maps 58"$\times$ 81" and the Na I magnetogram 31"$\times$ 81". The reduction procedure is the standard: correction for dark-current and flat-field, and also co-alignment.

3. Analysis

From the two data sets we have chosen for a detailed analysis four small elements, and studied their images, contour plots of the contrast of the images and the magnetic field intensity. We also have drawn the profiles of their values in two perpendicular directions to visualize their structure. Each of the sampled elements appear to have a different structure as may be expected from the turbulent nature of the atmospheric convection. Due to the different height formation of their radiation we see that the chromospheric Ca II H element images are generally wider than the G and CN bands due to the expansion of the flux tubes with height. Qu and Xu (2002) show that the Ca II radiation is generated in the chromosphere in quiet sun regions. Because of the space limitation we show only one of the four analyzed elements, corresponding to the Aug 7 dataset. In Fig. 1 from the upper-left corner and in clockwise direction, CN, Ca II, Na I magnetogram and G-band images are shown, two straight lines indicate the section through which we have cut the image to derive indicative profiles of the structure. The size of these images is 2"1 $\times$ 1"9.

In Fig. 2 the contours of relative intensity are plotted, in the same order of display as in Fig. 1. In the contours plots we identify a line of bright points in G-band and CN band indicating a sort of sheath magnetic field at photospheric level on the border of a granule, while at chromospheric level, the Na I magnetogram shows that the magnetic field bundle is largely expanded, expansion supported by the extension of the Ca II H image. Also, the South-North profile shows bumps in the G and CN bands, north of the peak in the magnetogram that would correspond to the well known effect of facular bright points resulting of seeing the outbound side of the magnetic field tube (the facula is located at μ=0.86).

Fig. 3 displays vertical profiles of the three images and the Na I magnetogram in two perpendicular planes, one along the West-East parallel and the other along the South-North meridian, both indicated in figure 1 by perpendicular lines. The scale is relative intensity in the left side of the plot, and the LOS-magnetogram V/I in the scale of the right side of the plot. It is interesting to notice that this bright structure is located at about μ=0.86, near the central North-South meridian. In the West-East plots, an

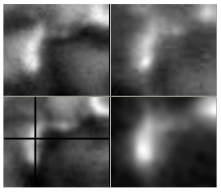

Figure 1. Case study of a facula. From upper-left corner in clockwise direction: CN, Ca II, Na I, G-band.

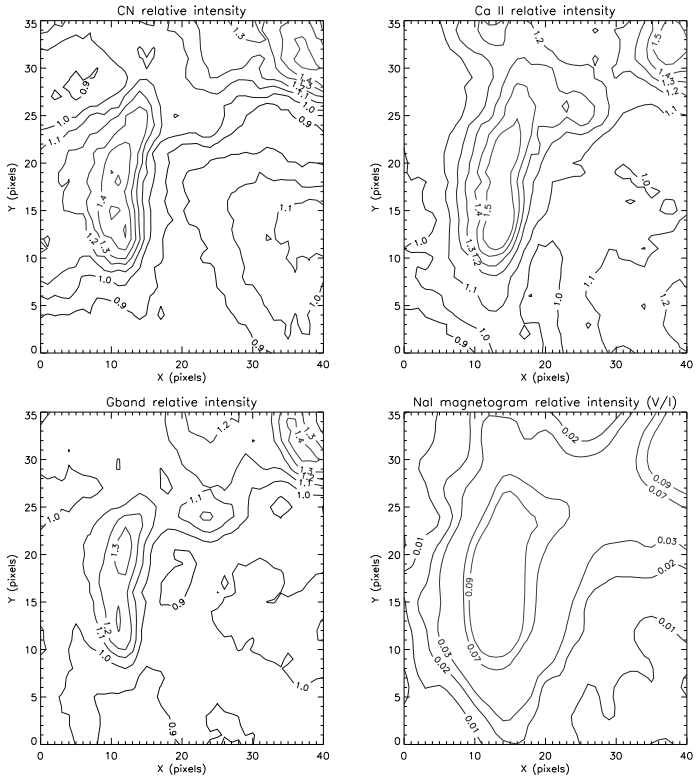

Figure 2. Relative intensity contours: CN, Ca II, Na I, G-band

asymmetry is noticeable from the Western facular point to the Eastern inter-granular lane and the adjacent granule.

4. Discussion and concluding remarks

Although this is only an example, we can say that the other three studied cases are also well represented by the expanding magnetic flux tube model with variations in their detailed structure, due to the diverse local convective structures, like one case in which there is evidence of the magnetic flux tube being inclined respect to the local vertical. It is worth reminding that we are studying the structure of an extremely dynamic environment. We can see, in general, that the CN band has higher contrast than the G-

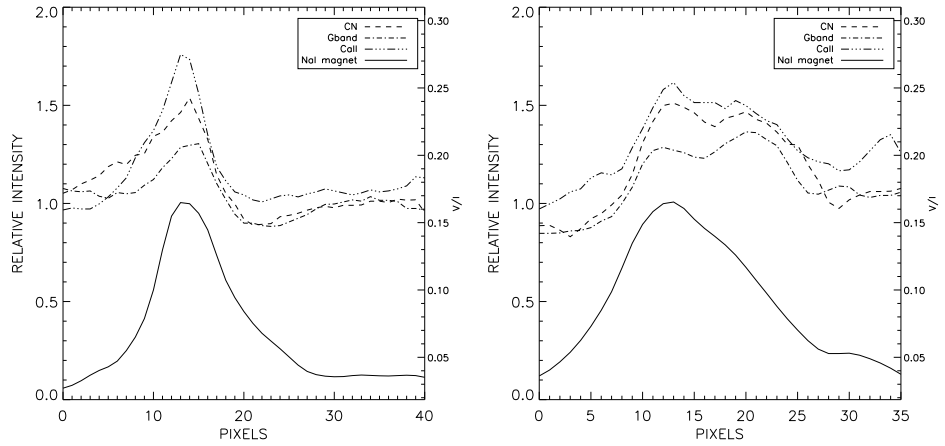

Figure 3. West-East (*left*) and North-South (*right*) relative intensity profiles. The scale on the right shows the V/I signal of the Na I magnetogram

band in the small magnetic elements, as was shown by Zakharov et al. (2005) in small magnetic elements in an active region. Due to the different height formation of their radiation we see that the Ca II H element images are generally wider than the G and CN bands due to the expansion of the magnetic flux bundle with height.

Acknowledgments. *Hinode* is a Japanese mission developed and launched by ISAS/JAXA, with NAOJ as domestic partner and NASA and STFC (UK) as international partners. It is operated by these agencies in co-operation with ESA and NSC (Norway).

References

Balmaceda, L. A., Palacios, J., Cabello I., Domingo, V., 2009, ASP Conference Series, 415, 156
Berger, T. et al., 2004, A&A, 428, 613
Bovelet, B., Wiehr., E., 2007, Sol.Phys., 243, 121-129
de Wijn, A. G, Stenflo, J. O., Solanki, S. K., Tsuneta, S., 2009, Space Sci.Rev.,144, 275
Kiselman, D., Rutten , R. J, Plez, B., 2001, IAU Symposium Vol 203, 287-290
Parker, E. N., 1976, ApJ, 204, 259
Qu, Z. Q., Xu, Z., 2002, Chin. J. Astron. Astrophys., 2(1), 71-80
Sánchez Almeida, J. 1997, ApJ, 491, 993
Sánchez Almeida, J., et al., 2004, ApJ, 609, L9
Spruit, H. C., 1976, Sol. Phys., 50, 269
Uitenbroek, H. & Tritschler, A., 2006, ApJ, 639, 525
Zakharov, V., et al., 2005, A&A, 437, L43